Journal of Solid Mechanics Vol. 4, No. 4 (2012) pp. 416-425

Frequency Response Analysis of a Capacitive Micro-beam Resonator Considering Residual and Axial Stresses and Temperature Changes Effects

S. Valilou*, M. Jalilpour

Department of Mechanical Engineering, Khoy Branch, Islamic Azad University, Khoy, Iran

Received 26 November 2012; accepted 28 December 2012

ABSTRACT

This paper presents a study on the frequency response of a capacitive micro-beam resonator under various applied stresses. The governing equation whose solution holds the answer to all our questions about the mechanical behavior is the nonlinear electrostatic equation. Due to the nonlinearity and complexity of the derived equation analytical solution are not generally available; therefore, the obtained differential equation has been solved by using a step by step linearization scheme and a Galerkin based reduced order model. The obtained static pull-in voltages have been validated by previous reports and a good agreement has been achieved. The dynamic behavior of the beam under residual, axial and thermal stresses has been investigated. It has been shown that applying the positive residual stress and negative temperature changes shifts right the frequency response and decrease the vibration amplitude and vice versa. Also, it has been shown that applying the bias DC voltage beside the exciting AC voltage decreases the stiffness of the system and so, shifts left the frequency response and increases the vibration amplitude.

Keywords: MEMS; Resonator; Residual stress; Axial stress; Temperature changes; Frequency response

1 INTRODUCTION

MICROELECTROMECHANICAL systems (MEMS) are increasingly gaining popularity in modern technologies, such as atomic force microscope (AFM), sensing sequence-specific DNA, and detection of single electron spin, mass sensors, resonators, chemical sensors, and pressure sensors [1-5]. MEMS devices are generally classified according to their actuation mechanisms. Actuation mechanisms for MEMS vary depending on the suitability to the application at hand. The most common actuation mechanisms are electrostatic, pneumatic, thermal, and piezoelectric. Electrostatically actuated devices form a broad class of MEMS devices due to their simplicity, as they require few mechanical components and small voltage levels for actuation [6], which the electrostatic actuation is inherently non-linear. Microbeam resonators (e.g., fixed-fixed and cantilever microbeam resonators) under voltage driving are widely used in many MEMS devices such as capacitive microswitches and resonant microsensors. These devices are fabricated, to some extent, in a more mature stage than some other MEMS devices. Fixed-fixed resonators due to their high natural frequencies are widely used in resonant sensors. One of the most important issues in the electrostatic actuated micro-devices is the pull-in instability. As the microstructure is balanced between electrostatic attractive force and mechanical (elastic) restoring force, both electrostatic and elastic restoring force are increased when the electrostatic voltage increases. When the voltage

* Corresponding author. Tel.: +98 9367469553; Fax: +98 4612553304.
E-mail address: svalilou@iaukhoy.ac.ir (S.Valilou).

reaches the critical value, pull-in instability happens. Pull-in is the point at which the elastic restoring force can no longer balance the electrostatic force. Increasing the voltage will cause the structure to have dramatic displacement jump further, which causes structure collapse and failure. Pull-in instability is a snap-through like behavior and it is saddle-node bifurcation type of instability [7]. In some devices such as micro-mirrors and micro-resonators, the designer avoids this instability to achieve stable motions, while in switching applications the designer exploits this effect to optimize device's performance.

Some previous studies predicted pull-in phenomena based on static analysis by considering static application of a DC voltage [8-11]. But there are not enough studies based on dynamic analysis by considering dynamic loading.

Beside the static pull-in, some researches introduced a dynamic pull-in voltage. Dynamic pull-in voltage is defined as a step DC voltage that when is applied suddenly, leads to the instability of the system [12].

On the other hand, one of the useful ways to study the resonators behavior is the frequency response analysis. Frequency response measurements can be used directly to quantify system performance and design control systems. In frequency response, analysis the excitation is explicitly defined in the frequency domain. Oscillatory loading is sinusoidal in nature. The steady-state oscillatory response occurs at the same frequency as the loading. The response may be shifted in time due to damping in the system. The shift in response is called a phase shift because the peak loading and peak response no longer occur at the same time.

Due to the frequency domain of this analysis other environmental conditions can also change the response by changing the stiffness and inertia of the system. In this paper, it is investigated the static and dynamic response of the fixed-fixed micro-beam resonators is investigated. Introducing a mathematical model, Galerkin-based step-by-step linearization method and reduced order model are used to solve the non-linear static and dynamic equations, respectively. The static problem is studied considering the effects of stretching, residual and thermal stresses. It is shown that these stresses affect the pull-in instability of the resonator. In the dynamic section, the frequency response of the resonator is studied. It is shown that applying the stresses shifts left and right the frequency response plot and changes the vibration amplitude.

2 MODEL DESCRIPTION AND MATHEMATICAL MODELING

Fig.1 shows a schematic view of a fixed-fixed beam resonator. Assume a beam with thickness h, width b, length L, density ρ and isotropic with Young's modulus E. Suppose that x is the coordinate along the length of the beam with its origin at the left end, and $w(x)$ is the transversal deflection of the beam, defined to be positive downward.

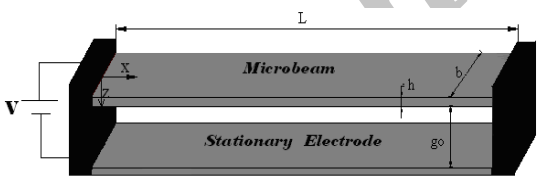

Fig. 1
Schematic of the fixed-fixed beam resonator.

Based on the static and dynamic behavior of electrostatic beam resonators subjected to non-uniform transverse electrostatic force, the governing equation can be expressed as [13]:

$$\tilde{E}I\frac{\partial^4 w}{\partial x^4}+\rho A\frac{\partial^2 w}{\partial t^2}+c\frac{\partial w}{\partial t}=\frac{\varepsilon b V^2}{2(g_0-w)^2} \tag{1}$$

where I is the moment of inertia of the cross-sectional area; ε is the dielectric coefficient (permittivity) of air; V is the applied voltage to the parallel beams and g_0 is the initial gap between them. For a wide beam, the effective modulus $\tilde{E}$ can be approximated by the plate modulus $E/(1-\upsilon^2)$; otherwise $\tilde{E}$ is the Young's modulus E, where ν is the Poisson's ratio of the micro-beam.

2.1 Residual stress

Considering the fabrication sequence of beam resonators, the residual stress is very important and inevitable to the device. Residual stress, owing to the mismatch of both thermal expansion coefficient and crystal lattice period between substrate and thin film, is unavoidable in surface micromachining techniques. Hence, accurate and reliable data of residual stress is important to the suitable design of the MEMS devices [14]. Therefore, the residual stress is a conspicuous research issue in the progress of the Microsystems Technology. The effective residual stress can be calculated as follow [15]:

$$\sigma_r = \sigma_0(1-\nu) \tag{2}$$

where σ_0 is the biaxial residual stress, σ_r is the effective residual stress. Hence, the effective axial force owing to the residual stresses can be obtained as [5]:

$$\int_{-h/2}^{+h/2} \sigma_r \, b \, dz = \sigma_r \, b \, h = T_r \tag{3}$$

2.2 Axial stress

When a fixed-fixed micro-beam is in tension, the actual beam length L' is longer than the original length L. Although there is no displacement in the x direction at the beam ends, hence the tensile stress due to bending generates an axial force [5]:

$$T_a = \sigma_a bh \cong \tilde{E} bh \frac{\Delta L}{L} \tag{4}$$

where: $\Delta L \cong \frac{1}{2}\int_0^L \left(\frac{dw}{dx}\right)^2 dx$

2.3 Temperature changes

The operating temperature of the flexible part of a beam resonator can be changed. These changes can occur owing to change of environmental temperature or due to heat generation because of intrinsic damping and power dissipation. Any change in the operating temperature of the flexible part, cause the coupled behavior of the MEMS resonator varies because the stress state is altered. Therefore, a full thermo-electro-mechanical analysis is required in identifying mechanical behavior and its implication on the resonator performance.

Due to microscale of the studied microbeam Biot number is much less than 0.1 so with a good acuracy temprature distribution can be assumed uniform [16]. Of course it must be noted that in microbeam or microplate resonators due to heat generation becaues of straine rate, a temprature gradirent will be created, but this case is not studied in this investigation**.** In the micro-beam due to its fixed boundary conditions, the thermal force due to the thermal stress in longitudinal direction can be expressed as [5]:

$$T_T = \tilde{E}\alpha \, \Delta T(bh) \tag{5}$$

2.4 Governing equation

The governing differential equation of micro-beam motion considering effects of residual and axial stresses and temperature changes can be expressed as:

$$\tilde{E}I \frac{\partial^4 w}{\partial x^4} - [T_r + T_a + T_T] \frac{\partial^2 w}{\partial x^2} + \rho A \frac{\partial^2 w}{\partial t^2} + c \frac{\partial w}{\partial t} = \frac{\varepsilon b V^2}{2(g_0 - w)^2} \tag{6}$$

The boundary conditions for the fixed-fixed micro-beam are defined as below:

$$w(l,t)=0 \quad , \quad \frac{\partial w}{\partial x}\Big|_{x=l}=0$$
$$w(0,t)=0 \quad , \quad \frac{\partial w}{\partial x}\Big|_{x=0}=0 \tag{7}$$

In order to non-dimensionalize Eq. (6) following non-dimensional parameters is introduced:

$$\hat{w}=\frac{w}{g_0};\hat{x}=\frac{x}{L};\hat{t}=\frac{t}{t^*} \qquad with \qquad t^*=\sqrt{\frac{\rho bhL^4}{\tilde{E}I}} \tag{8}$$

Using these non-dimensional parameters Eq. (6) takes the following form:

$$\frac{\partial^4\hat{w}}{\partial\hat{x}^4}-[D_1+D_2\int_0^1(\frac{\partial\hat{w}}{\partial\hat{x}})^2d\hat{x}+D_3]\frac{\partial^2\hat{w}}{\partial\hat{x}^2}+\frac{\partial^2\hat{w}}{\partial\hat{t}^2}+D_4\frac{\partial\hat{w}}{\partial\hat{t}}=D_5\frac{V^2}{(1-\hat{w}\ )^2} \tag{9}$$

where

$$D_1=\frac{12\sigma_r L^2}{Eh^2}\ ;\quad D_2=\frac{6g_0^2}{h^2}\ ;\quad D_3=\frac{12\alpha\Delta TL^2}{h^2}\ ;\ D_4=\frac{12cL^4}{\tilde{E}bh^3t^*}\ ;\ D_5=\frac{6\varepsilon L^4}{\tilde{E}h^3g_0^3} \tag{10}$$

In order to study the micro-beam motion about a statically deflected position total deflection of the microbeam can be expressed as:

$$\hat{w}(x,t)=\hat{w}_s(x)+\hat{w}_d(x,t) \tag{11}$$

Assuming that a bias tuning DC voltage is applied statically, which cause the inertial terms to be vanished; Eq. (6) defining static deflection of the microbeam takes the following form:

$$\frac{d^4\hat{w}_s}{d\hat{x}^4}-[D_1+D_2\int_0^1(\frac{d\hat{w}_s}{d\hat{x}})^2d\hat{x}+D_3]\frac{d^2\hat{w}_s}{d\hat{x}^2}=D_5\frac{V^2}{(1-\hat{w})^2} \tag{12}$$

By eliminating equation of static deflection from Eq.(6) and linearizing electrostatic nonlinear force using Calculus of Variation Theory and Taylor series expansions about static deflection the dynamic equation of small motion about the statically deflected position takes the following form:

$$\frac{\partial^4\hat{w}_d}{\partial\hat{x}^4}-(D_1+D_2\int_0^1(\frac{\partial\hat{w}_s}{\partial\hat{x}})^2d\hat{x}+D_3)\frac{\partial^2\hat{w}_d}{\partial\hat{x}^2}+\frac{\partial^2\hat{w}_d}{\partial\hat{t}^2}+D_4\frac{\partial\hat{w}_d}{\partial\hat{t}}-D_5\frac{V_{dc}^2}{(1-\hat{w}_s)^3}\hat{w}_d=2D_5\frac{V_{dc}}{(1-\hat{w}_s)^2}V_{ac} \tag{13}$$

3 NUMERICAL SOLUTION

3.1 Static deflection analysis

In capacitive tunable resonators owing to an applied DC voltage, governing equation of static deflection can be expressed as Eq.(12). Because of nonlinearity of this equation, the solution is complicated and time consuming, so in order to solve it, it is tried to linearize it. Because of considerable value of $\hat{w}_s$ respect to initial gap especially when the applied bias DC voltage is increased, the linearizing respect to the initial position may cause to appear some considerable errors. Therefore, to minimize the value of errors, a step by step increasing the applied voltage is proposed. In order to use step by step linearization method (SSLM), $\hat{w}_s^i$ is considered the micro-beam deflection

due to an applied voltage V_i, hence a small increase of the applied voltage leads to a small change in the microbeam deflection [5]:

$$\hat{w}_s^{i+1} \to \hat{w}_s^i + \Psi_s(x) \tag{14}$$

when

$$V_{i+1} \to V_i + \Delta V \tag{15}$$

For step i, the Eq. (12) is written as:

$$\frac{\partial^4 \hat{w}_s^i}{\partial \hat{x}^4} - [D_1 + D_2 \int_0^1 (\frac{\partial \hat{w}_s^i}{\partial \hat{x}})^2 d\hat{x} + D_3] \frac{\partial^2 \hat{w}_s^i}{\partial \hat{x}^2} = D_5 \frac{V_i^2}{(1-\hat{w}_s^i)^2} \tag{16}$$

Eq. (12) can be rewritten in *i+1* step as follow:

$$\frac{\partial^4 \hat{w}_s^{i+1}}{\partial \hat{x}^4} - [D_1 + D_2 \int_0^1 (\frac{\partial \hat{w}_s^{i+1}}{\partial \hat{x}})^2 d\hat{x} + D_3] \frac{\partial^2 \hat{w}_s^{i+1}}{\partial \hat{x}^2} = D_5 \frac{V_{i+1}^2}{(1-\hat{w}_s^{i+1})^2} \tag{17}$$

Substituting Eqs. (14, 15) into Eq. (17), we have:

$$\frac{\partial^4 (\hat{w}_s^i + \Psi_s(x))}{\partial \hat{x}^4} - [D_1 + D_2 \int_0^1 (\frac{\partial (\hat{w}_s^i + \Psi_s(x))}{\partial \hat{x}})^2 d\hat{x} + D_3] \frac{\partial^2 (\hat{w}_s^i + \Psi_s(x))}{\partial \hat{x}^2} = D_5 \frac{V_{i+1}^2}{(1-\hat{w}_s^i - \Psi_s)^2} \tag{18}$$

Using Taylor's series expansion about $\hat{w}_s^i$ and applying the truncation to first order, the linear coupled electrostatic forces can be written as:

$$\frac{\partial^4 (\hat{w}_s^i + \Psi_s(x))}{\partial \hat{x}^4} - [D_1 + D_2 \int_0^1 (\frac{\partial (\hat{w}_s^i + \Psi_s(x))}{\partial \hat{x}})^2 d\hat{x} + D_3] \frac{\partial^2 (\hat{w}_s^i + \Psi_s(x))}{\partial \hat{x}^2} = \frac{D_5 V_{i+1}^2}{(1-\hat{w}_s^i)^2} + \frac{2D_5 V_{i+1}^2}{(1-\hat{w}_s^i)^3} \Psi \tag{19}$$

By substituting Eq. (19) into Eq. (18), the following equation can be obtained to calculate Ψ_s:

$$\frac{d^4 \Psi_s}{d\hat{x}^4} - \left[D_1 + D_2 \int_0^1 \left(\frac{d\hat{w}_s^i}{d\hat{x}} \right)^2 d\hat{x} + D_3 \right] \frac{d^2 \Psi_s}{d\hat{x}^2} - \frac{2D_5 V_{i+1}^2}{(1-\hat{w}_s^i)^3} \Psi_s = \frac{D_5}{(1-\hat{w}_s^i)^2} (V_{i+1}^2 - V_i^2) \tag{20}$$

The obtained linear differential equation is solved by Galerkin method. $\Psi(\hat{x})$ based on function spaces can be expressed as [5]:

$$\Psi(\hat{x}) = \sum_{j=1}^{\infty} a_j \, \phi_j(\hat{x}) \tag{21}$$

In this paper, $\phi_j(\hat{x})$ is selected as *j*th undamped linear mode shape of the straight microbeam. The unknown $\Psi(\hat{x})$, is approximated by truncating the summation series to a finite number, *n*:

$$\Psi_n(\hat{x}) = \sum_{j=1}^{n} a_j \, \phi_j(\hat{x}) \tag{22}$$

Substituting the Eq. (22) into Eq.(20), and multiplying by $\phi_i(\hat{x})$ as a weight function in Galerkin method and then integrating the outcome from $\hat{x} = 0$ to 1, a set of linear algebraic equation is generated as:

$$\sum_{j=1}^{n} K_{ij} a_j = F_i \qquad i = 1,...,n \tag{23}$$

where $K_{ij} = K_{ij}^{\ m} + K_{ij}^{\ a} - K_{ij}^{\ e}$ and:

$$\begin{aligned}
K_{ij}^{\ m} &= \int_0^1 \phi_i \phi_j^{\ iv} d\hat{x} \\
K_{ij}^{\ a} &= -\int_0^1 \phi_i \left(\left(\left[D_1 + D_2 \int_0^1 \left(\frac{d\hat{w}_s^i}{d\hat{x}} \right)^2 d\hat{x} + D_3 \right] \right) \varphi_j'' \right) \\
K_{ij}^{\ e} &= \frac{2D_5 V_{i+1}^2}{(1-\hat{w}_s^i)^3} \int_0^1 \phi_i \phi_j d\hat{x} \\
F_i &= \frac{D_5}{(1-\hat{w}_s^i)^2} (V_{i+1}^2 - V_i^2) \int_0^1 \phi_i(\hat{x}) d\hat{x}
\end{aligned} \tag{24}$$

3.2 Frequency response analysis

For studying the fixed-fixed microbeam response to dynamic loading a Galerkin-based reduced order model can be used [23]. Because of the non-linearity of electrostatic force and stretching terms, direct applying of reduced order model to dynamic equation Eq. (13) leads to generation of *n* nonlinear coupled ordinary differential equation and consequently the solution is more complicated. To solve this difficulty, the hardening *($\hat{N}_a$)* and forcing term in Eq. (13) are considered a constant term in each time step of integration and takes the value of previous step. By selecting small enough time steps this assumption leads to accurate enough results. Now Eq. (13) can be rewritten as following:

$$\frac{\partial^4 \hat{w}}{\partial \hat{x}^4} + \frac{\partial^2 \hat{w}}{\partial \hat{t}^2} + D_4 \frac{\partial \hat{w}}{\partial \hat{t}} - \left[D_1 + D_2 \int_0^1 \left(\frac{d\hat{w}_s^i}{d\hat{x}} \right)^2 d\hat{x} + D_3 \right] \frac{\partial^2 \hat{w}}{\partial \hat{x}^2} - D_5 \frac{V_{dc}^2}{(1-\hat{w}_s)^3} \hat{w}_d = 2 D_5 \frac{V_{dc}}{(1-\hat{w}_s)^2} V_{ac} \tag{25}$$

To achieve a reduced order model, $\hat{w}(\hat{x},\hat{t})$ can be approximated as [5]:

$$\hat{w}(\hat{x},\hat{t}) = \sum_{j=1}^{n} U_j(\hat{t}) \phi_j(\hat{x}) \tag{26}$$

By substituting the Eq. (26) into Eq.(25) and multiplying by $\phi_i(\hat{x})$ as a weight function in Galerkin method and then integrating the outcome from $\hat{x} = 0$ to 1, the Galerkin based reduced order model is generated as:

$$\sum_{j=1}^{n} M_{ij} \ddot{T}_j(\hat{t}) + \sum_{j=1}^{n} C_{ij} \dot{T}_j(\hat{t}) + \sum_{j=1}^{n} \left[K^m + K^a - K^e \right] T_j(\hat{t}) = F_i \tag{27}$$

where $\boldsymbol{M}, \boldsymbol{C}, \boldsymbol{K^m}$ and $\boldsymbol{K^a}$ are mass, damping, mechanical and axial stiffness matrices, respectively. Also $\boldsymbol{F}$ introduces the forcing vector. The mentioned matrices and vector are given by:

$$M_{ij} = \int_0^1 \phi_i \phi_j d\hat{x} \qquad i, j = 1, \ldots, n$$

$$C_{ij} = D_4 \int_0^1 \phi_i \phi_j d\hat{x}$$

$$K_{ij}^m = \int_0^1 \phi_i \phi_j{}^{iv} d\hat{x}$$

$$K_{ij}^a = -\left[D_1 + D_2 \int_0^1 \left(\frac{d\hat{w}_s^i}{d\hat{x}} \right)^2 d\hat{x} + D_3 \right] \int_0^1 \phi_i \varphi''_j d\hat{x} \tag{28}$$

$$F_i = \int_0^1 2 D_5 \frac{V_{dc}}{(1-\hat{w}_s)^2} V_{ac} \phi_i d\hat{x}$$

$$K_{ij}^e = D_5 \frac{V_{dc}^2}{(1-\hat{w}_s)^3} \int_0^1 \phi_i \phi_j d\hat{x}$$

Now, Eq. (27) can be integrated over time by various integration methods such as Runge-Kutta method.

4 NUMERICAL RESULTS AND DISCUSSION

For verification of our numerical solution it is considered a microbeam with the geometric and material properties listed in Table 1.

Table 1
The values of design variables

Design Variable	Value
b	$50\ \mu m$
h	$3\ \mu m$
d	$1\ \mu m$
E	$169\ GPa$
ρ	$2331\ kg/m^3$
ε	$8.85\ PF/m$
ν	0.06

Table 2
Comparsion of the Pull-in Voltage for a fixed-fixed microbeam

	Residual stress *(MPa)*	Our results	Energy model [11]	MEMCAD [11]
$L = 350\ \mu m$	0	$20.1 V$	$20.2\ V$	$20.3\ V$
	100	$35.3\ V$	$35.4\ V$	$35.8\ V$
	-25	$13.8\ V$	$13.8\ V$	$13.7\ V$
$L = 250\ \mu m$	0	$39.5\ V$	$39.5\ V$	$40.1\ V$
	100	$57.3\ V$	$56.9\ V$	$57.6\ V$
	-25	$33.4\ V$	$33.7\ V$	$33.6\ V$

In Table 2 it is compared the calculated pull-in voltage with previous works for the fixed-fixed and cantilever microbeams with properties of Table 1, respectively. It is shown that the calculated pull-in voltages are in good agreement with previous works. Figs. 2, 3 and 4 show the effects of the stretching, residual and thermal stresses on the variation of the fundamental frequency of the micro-beam, respectively. As shown the frequency varies from the value for the un-loaded beam to zero by increasing the DC voltage from zero to the pull-in voltage. Also, the figures show that applying the tensile forces increases the frequency and pull-in voltage of the beam and vice versa.

In following it is investigated the effects of the residual and thermal stresses on the frequency response of the beam resonator with $L = 350\ \mu m$.

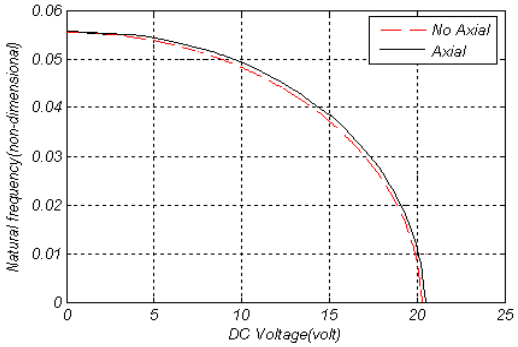

Fig. 2
Variation of the fundamental frequency versus applied DC voltage with and without stretching $(T_r = 0,\ \Delta T = 0)$.

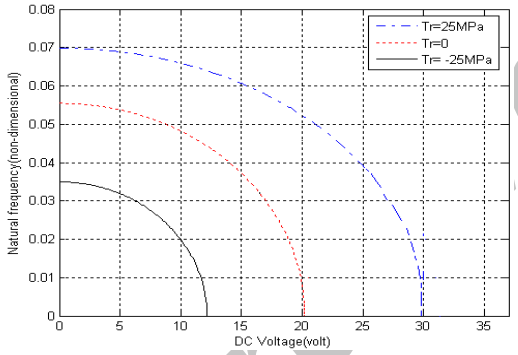

Fig. 3
Variation of the fundamental frequency versus applied DC voltage for different residual stresses $(T_a = 0,\ \Delta T = 0)$.

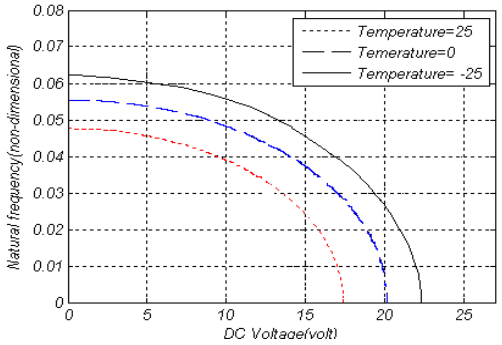

Fig. 4
Variation of the fundamental frequency versus applied DC voltage for different temperature changes $(T_r = 0,\ T_a = 0)$.

In Fig. 5 the frequency response of the beam resonator under various residual stresses is plotted. As shown the tensile stress shifts right the response and decreases the amplitude and vice versa. Fig. 6 shows the response for positive and negative temperature changes. As illustrated, increasing the temperature of the resonating beam

decreases the resonance frequency and increases the amplitude. On the other hand, decreasing the temperature shifts right the response and decreases the amplitude of the resonance.

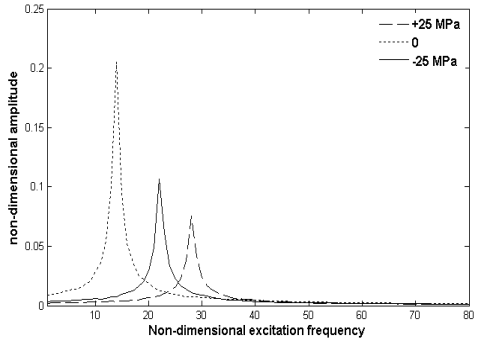

Fig. 5
Frequency response with considering different value of residual stress.

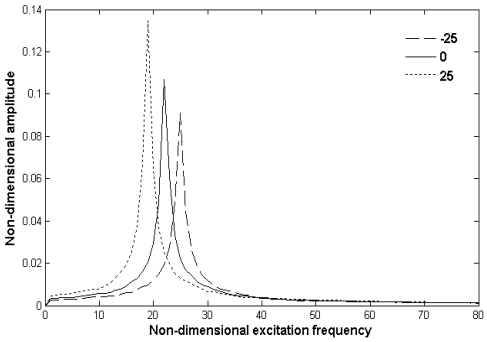

Fig. 6
Frequency response with considering different value of Temperature changes.

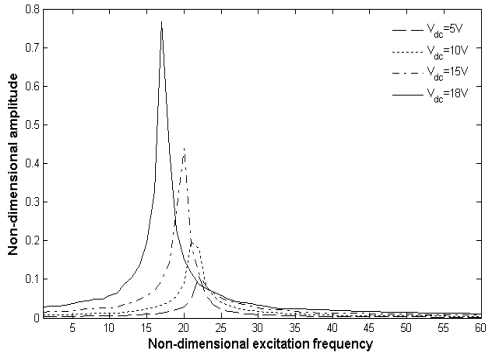

Fig. 7
Frequency response with considering different value of the applied bias voltage.

Fig. 6 shows that applying a positive temperature change shifts left the diagram and decreases the vibration amplitude. This is due to the decrease of the stiffness and consequently the natural frequency of the beam. Also, as shown the negative temperature change increases the natural frequency and decreases the amplitude. Finally, in Fig. 7 the effects of the applied bias voltage on the frequency response are shown. As obtained, increasing the bias voltage increases the electrical stiffness and decreases the total stiffness of the beam and consequently decreases the fundamental frequency and increases the vibration amplitude of the beam.

5 CONCLUSIONS

In the presented paper, the static and dynamic behavior of a capacitive micro-beam resonator was studied considering the residual stress from fabrication processes, the nonlinear stretching stress effects due to beam deflection and the thermal stress due to the temperature changes. Because of the nonlinearity and complexity of the derived equation, a numerical step by step linearization scheme and a Galerkin based reduced order model were used to solved the static and dynamic equations, respectively. Due to the importance of the frequency analysis in the resonator behavior, the frequency response of the beam was plotted for different values of the residual and thermal stresses. It was shown that applying the tensile stresses shifts right the frequency response and decreases the vibration amplitude and vice versa. Also, the effect of the applied bias voltage on the frequency response was studied. It was shown that increasing the bias voltage decreases the stiffness of the system and consequently shifts left the frequency response and increases the vibration amplitude. Finally, it can be conclude that the behavior of the resonators can be varied and controlled by some external mechanical parameters.

REFERENCES

[1] Basso M., Giarre L., Dahleh M., Mezic I., 1998, Numerical analysis of complex dynamics in atomic force microscopes*, Proceedings of the IEEE International Conference on Control Applications* ***2****:*1026–1030.

[2] Fritz J., Baller M.K., Lang H.P., Rothuizen H., Vettiger P., Meyer E., Gntherodt H.J., Gerber C., Gimzewski J.K., 2001,Translating bio-molecular recognition into nanomechanics , *Science* **288**:316–318.

[3] Sidles JA., 1991, Noninductive detection of single proton-magnetic resonance, *Applied Physics Letters* **58**:2854-2856.

[4] Nabian A., Rezazadeh G., Haddad-derafshi M., Tahmasebi A., 2008, Mechanical behavior of a circular micro plate subjected to uniform hydrostatic and non-uniform electrostatic pressure, *Microsyst Technol* **14**:235–240.

[5] Fathalilou M., Motallebi A., Rezazadeh G., Yagubizade H., Shirazi K., Alizadeh Y., 2009, Mechanical Behavior of an Electrostatically-Actuated Microbeam under Mechanical Shock, *Journal of Solid Mechanics* **1**: 45-57.

[6] Senturia SD., 2001, *Microsystem Design, Norwell*, MA: Kluwer.

[7] Zhang Y., Zhao Y., 2006, Numerical and analytical study on the pull-in instability of micro- structure under electrostatic loading, *Sensors and Actuators A: Physical* **127**: 366-367.

[8] Rezazadeh G., Sadeghian H., Abbaspour E., 2008, A comprehensive model to study nonlinear behaviour of multilayered micro beam switches, *Microsyst Technol* **14**: 143.

[9] Sadeghian H., Rezazadeh G., 2007, Application of the Generalized Differential Quadrature Method to the Study of Pull-In Phenomena of MEMS Switches, *Journal of Microelectromechanical Systems* **16**(6):1334-1340.

[10] Osterberg P.M., Senturia S.D., 1997, M-TEST a test chip for MEMS material property measurement using electrostatically actuated test structures, *Journal of Microelectromechanical Systems* **6**(2):107-118.

[11] Senturia SD., Aluru N, White J., 1997, Simulating the behavior of MEMS devices, *IEEE Computing in Science and Engineering* **4**(1): 30–43.

[12] Abdel-Rahman E.M., Younis M.I., Nayfeh A.H., 2002, Characterization of the mechanical behavior of an electrically actuated microbeam , *Journal of Micromechanics and Microengineering* **12**:759–766.

[13] Rezazadeh G., Tahmasebi A., Zubtsov M., 2006, Application of Piezoelectric Layers in Electrostatic MEM Actuators: Controlling of Pull-in Voltage, *Microsyst Technol* **12** : 1163-1170.

[14] Mukherjee T., Fedder G.K., White J., 2000, Emerging simulation approaches for micromachined devices, *IEEE Transactions on Computer- Aided Design of Integrated Circuits and Systems* **19**: 1572–1589.

[15] Senturia SD., 1998, CAD challenges for microsensors, microactuators, and Microsystems, *Proceedings of the IEEE* **86**: 1611–1626.

[16] Talebian S., Rezazadeh G., Fathalilou M., Yagubizade H., 2010, Effect of Temperature on Pull-in Voltage and Natural Frequency of an Electrostatically Actuated Microplate, *Mechatronics* **20**(6):666-673.